Quantitative Visualization of Transient Heat Transfer of Oblique Impinging Jet Using Thermographic Phosphor

Mirae Kim[1], Dong Kim[1], Seung Jae Yi[2], Hyun Dong Kim[1], Kyung Chun Kim[1,*]

[1]School of Mechanical Engineering, Pusan National University, Busan, Korea
[2]Propulsion Test and Evaluation Team, Korea Aerospace Research Institute, Daejeon, Korea
*corresponding author: kckim@pusan.ac.kr

Abstract The transient heat transfer and flow characteristics of oblique impinging jets, according to the impinging angle and distance from nozzle to the plate were studied. To investigate the temperature change of the hot plate, thermographic phosphor thermometry was used. For the transient heat transfer analysis, 1D semi-infinite solid model was used to obtain a coefficient of local heat transfer and Nusselt number. The peak heat transfer was occurring at the stagnation point, and secondary peak was also occurred at the low distance from nozzle to plate and high impinging angle condition. These secondary peaks are shown to be due to an abrupt increase in turbulence in the wall jet boundary layer. In order to verify this phenomenon, we conducted a flow visualization of oblique impinging jets on the hot plate
Keywords: Heat transfer, Oblique impinging jet, Thermographic phosphor, Thermometry, Flow visualization

1 Introduction

Impinging jet has effect on high heat and mass transfer locally, so it is used in various industrial fields. In particular, impinging jet is used in various areas including heat treatment of metal [1], cooling of turbine blade [2], local cooling and press work of electronic components [3] and drying process in glass industries. In addition to this, it is economical because it helps to transfer high heat locally. The primary purpose of heat transfer study by impinging jet is to maximize heat and mass transfer ultimately. In this regard, study on variables including nozzle shape [4, 5], exit condition [6], Reynold number , the distance between nozzle and impinging plate [7] and curvature of impinging surface [8] has been conducted.

In research on impinging jet, thermocouple or heat flux gage has been generally used to analyze a heat transfer characteristics. Such sensors have high accuracy to obtain data, but have lower spatial resolution, because only point measurement is practicable. Complicated measurement devices are needed to analyze heat transfer in a large area. Whereas, optical measurement technique has higher spatial resolution compared to the existing point measurement technique. Moreover, optical measurement technique is non-interference measurement technique that measurement devices do not affect flow, so its analysis can be carried out more accurately.

Liquid crystal, IR camera and TSP (Temperature sensitive paint) techniques are generally used as one of the techniques of two-dimensional optical temperature measurement. However, some techniques, such as Liquid crystal and TSP, are limited to cover variety range of temperature and they can be only applied at lower temperature under 200℃. IR camera can be applied at high temperature, but it has its limitation to measure accurate temperature, because emissivity varies depending on the changes of temperature. On the other hand, temperature measurement technique using thermographic phosphors can measure the accurate 2D temperature field even in the harsh environment such as high temperature and high pressure, because it is

not affected by oxygen quenching or pressure up to 10 bar [9].

For these reasons, the heat transfer characteristics as the impinging angle were studied with the thermographic phosphor system which could obtain the 2D temperature field with high accuracy. The instantaneous temperature fields with 0.1 second interval are quantitatively measured using thermographic phosphor, and the characteristics of transient heat transfer are investigated.

2 Theoretical background

2.1 Thermographic phosphor

There are a variety of thermographic phosphors, so proper thermographic phosphor needs to be selected depending on the range of measure temperature and analysis method. In this study, Mg4FGeO6:Mn is selected as thermographic phosphor, because it has relatively continuing characteristic of phosphorescence while it can measure at a wide range of temperature [10]. Mg4FGeO6:Mn is thermographic phosphor which can measure temperature at the range of 13 K ~ 1000 K [11, 12]. Manganese ion absorbs ultraviolet range of 385 nm and emits fluorescence of 650 nm wavelength (Blasse and Grabmaier, 1994). Brubach et al. investigated the fluorescent characteristic of Mg4FGeO6:Mn on the dopant concentration, the laser pulse energy, gas composition, pressure effects and irreversible change by heat treatment. According to their research, decay time characteristic of Mg4FGeO6:Mn is affected by dopant concentration, power of laser pulse and maximum temperature of heat treatment, but not affected by gas composition and pressure. However, considering their research results, influence by dopant concentration or laser power could be removed by using the same test piece and light source at the calibration and experiment. In this study, such errors have been removed as using same test piece both calibration experiment and the experiment of impinging jet.

2.2. Decay-slope analysis method

Generally, intensity based method and temporal signal based method are used as one of the temperature field analysis method using thermographic phosphors. Absolute intensity method is analysis method based on the characteristic of changing fluorescence intensity depending on the concentration of quencher, but it needs to be controlled, because signal can be differ by other factors such as uniformity of illumination, concentration of phosphor. In order to improve accuracy of absolute intensity method, intensity ratio method is suggested [13]. Compared to absolute intensity method, intensity ratio method has higher accuracy, but its measurement system is complicated.

Temporal signal based method is analysis method using characteristic of emission of phosphor with time, and lifetime analysis and rise-time analysis are generally used. Compared to intensity method, temporal signal based method has higher accuracy, but it takes long time to analyze [14]. In this regards, Yi et al. suggested decay-slope analysis method as a new analysis method using temporal signal [15], and it is based

on the phosphorescence signal with time in equation (1).

$$V(t) = Ae^{\frac{t}{\tau}} + b + \varepsilon(t) \tag{1}$$

where *A* and *b* are the initial intensity and baseline offset, τ and *t* are the lifetime and time, and $\varepsilon(t)$ is noise term generated by shot noise, quantization noise and background radiation. The noise term $\varepsilon(t)$ can be reduced by averaging repeated experiments, and in case of be known baseline term (*b*) a priori, equation 1 can be rewritten as

$$I(t) = Ae^{-\frac{t}{\tau}} \tag{2}$$

where $I(t)=V(t)-b$. The normalized intensity which was obtained by intensity $I(t)$ divided by initial intensity (I_0) can eliminate the some error terms, such as non-uniform light source/phosphor concentration and shot-to-shot fluctuation .

$$\frac{I(t)}{I_0} = A' e^{-\frac{t}{\tau}} \tag{3}$$

The phosphorescence lifetime could be estimated using nonlinear least-squares approximation algorithm to the equation 3, respectively. The Trust-Region algorithm was used to obtain the lifetime constant, and lifetime constant is consisted by decay constant (λ)

$$\lambda = \frac{1}{\tau} \tag{4}$$

Equation (3) can be summarized by decay slope constant λ and log-scale term

$$\frac{I(t)}{I_0} = A' e^{\lambda t} \tag{5}$$

$$ln\left(\frac{I_0}{I(t)}\right) = \lambda t + ln\left(A'\right) \tag{6}$$

where λ and A' could be estimated using linear least-squares curve fitting. According to equation (6), the ratio of intensity between I_0 and $I(t)$ and time *t* has a linear relationship with the slope of decay constant λ.

2.3 Transient heat transfer analysis

Transient heat transfer measurement technique is method to obtain a coefficient of heat transfer assuming thermographic phosphor coated test surface as one-dimensional semi-infinite solid model having convective boundary condition and using temperature change of the surface with time as giving sudden change to temperature and velocity of the mainstream. The 1D conduction equations on the thermographic phosphor coated surface is:

$$k\frac{\partial^2 T}{\partial x^2} = \rho C_P \frac{\partial T}{\partial t} \tag{7}$$

initial condition and boundary conditions:

at $t = 0$, $T = T_i$

at $x = 0$, $-k\frac{\partial T}{\partial x} = h(T_w - T_m)$

at $x \to \infty$, $T = T_i$

In general, when surface heated at constant temperature is cooled by impinging jet, local h could be obtained by equation (7). The non-dimensional temperature at the convection boundary layer (at x = 0) could be obtained by solving equation (7) with initial and boundary conditions.

$$\frac{T_w - T_i}{T_m - T_i} = 1 - \exp\left(\frac{h^2 \alpha t}{k^2}\right) erfc\left(\frac{h\sqrt{\alpha t}}{k}\right) \tag{8}$$

3 Experimental apparatus and calibration curve

Fig. 1 shows the experimental apparatus for the calibration and experiment. The Mg_4FGeO_6:Mn was coated on the aluminum plate using HPC chemical binder (ZYP Coatings, Inc.), and it was placed on a hot plate (Corning PC-600D) which could control the temperature up to 550 ℃. A K type thermocouple was used to monitor the temperature of the target plate. The glass chamber made from tempered glass was installed to cover the hot plate system to prevent the effect of ambient air flow to an aluminum plate. To illuminate the manganese ion in Mg_4FGeO_6:Mn, a ultraviolet LED (Prizmatix, UHP-T-LED-385), which has around 0.2 mJ per pulse and 385 nm wavelength was used. The phosphorescence image from thermographic phosphor was obtained using a high speed camera (Photron SA 1.1) with 4000 frame per second. A narrow band-pass filter around 655 ± 20 nm wavelength (Edmundoptics, #67-051) was mounted on a 50 mm lens (Canon 50 mm f/1.2) to obtain only the luminescence signal. A function generator was used to control the start timing of the UV-LED and high speed camera, and air compressor used to supply compressed air for impinging jet. Therefore, the distribution of instantaneous temperature with 0.1 second interval is quantitatively measured with this experimental setup.

Fig. 2 shows layout of thermoraphic phosphor coated layer, field of view and the location of nozzle. The Mg_4FGeO_6:Mn was coated on a 69 mm × 69 mm area in the center of a 120 mm ×120 mm aluminum plate. The field of view was 65 × 65 mm of TP coated layer, and the image resolution is 0.0927 mm/pixel. The inner diameter of the nozzle was 2 mm, and the jet Reynolds number was fixed at 3500. The distance between nozzle to plate (H/D) was changed from 4 to 8, and impinging angle (α) was also changed. The instantaneous temperature fields were obtained for 2.8 seconds, and the transient heat transfer characteristic was investigated with different H/D and impinging angle.

The calibration was performed from 350 ~ 630 K with 30 K intervals. The decay-slope analysis method was used to convert decay-slope constant to temperature, and Fig. 3 shows the represented decay-slope constant and a calibration curve. The 3rd order polynomial curve fitting was used to obtain a calibration

curve, and the adjusted R-square which could indicate the goodness of fit was 99.9 %. The decay-slope constant is increased when calibration temperature increasing. The surface temperature on the aluminum plate was calculated with this calibration results.

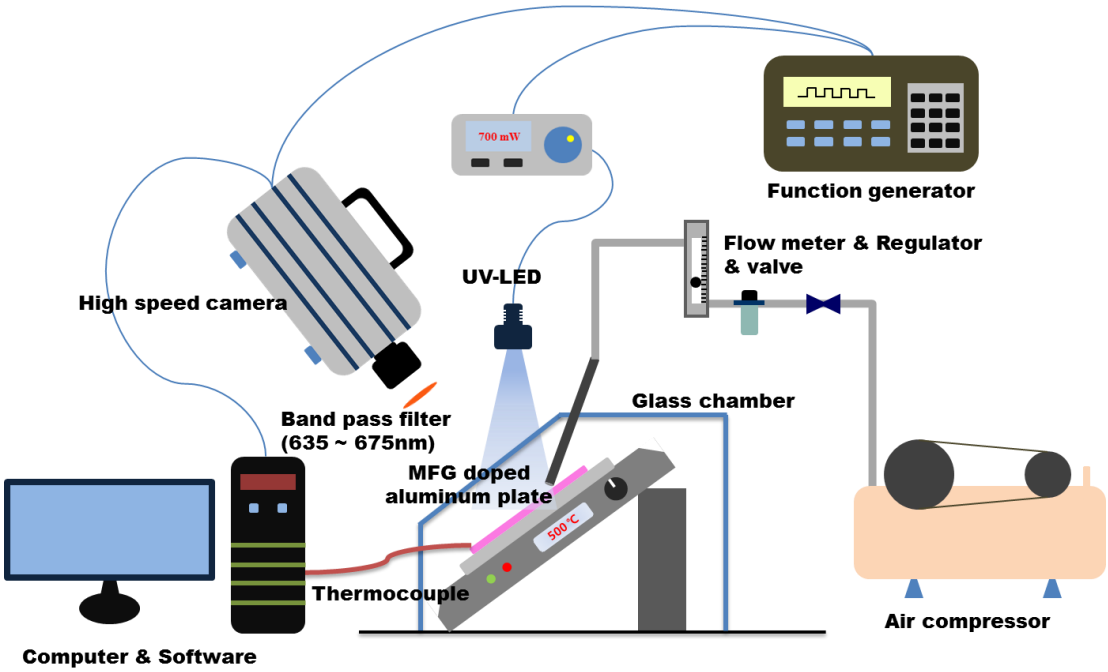

Fig. 1. Experimental setup

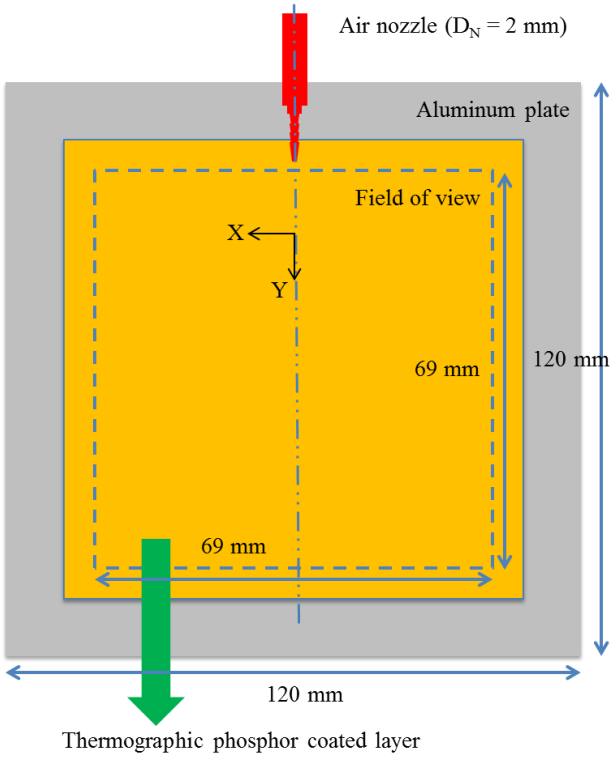

Fig. 2. The schematic of thermographic phosphor coated layer, field of view and the location of air nozzle

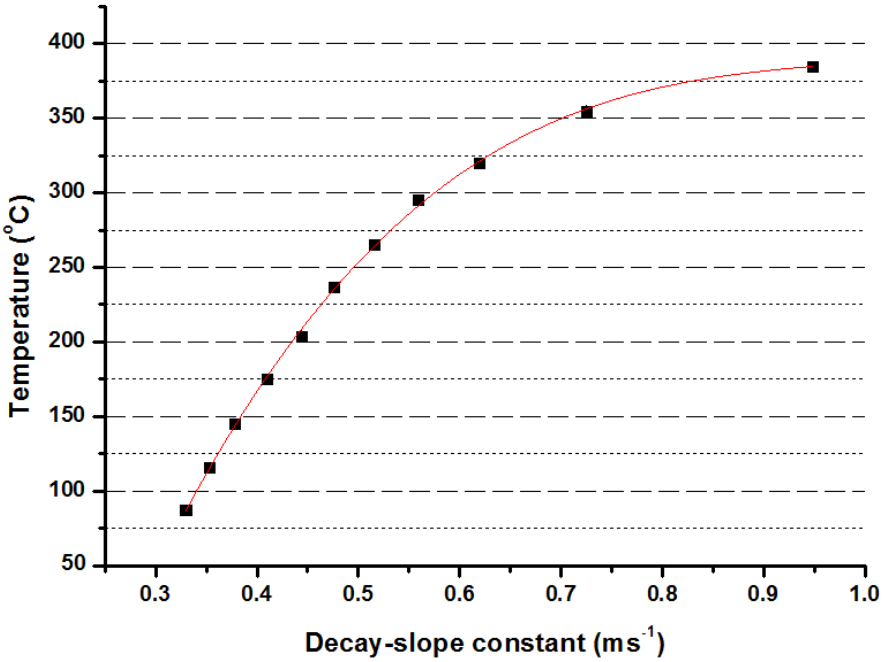

Fig. 3. Calibration curve of temperature-Decay slope constant

4 Results and discussion

4.1 2-dimensional temperature distribution on the hot plate

The instantaneous temperature fields were shown in Fig. 4. Fig. 4 shows the instantaneous temperature field at H/D=4, α=30°. The nozzle and its shade appeared at the bottom side. Before the impinging jet starting, the surface temperature remained around 360℃, and temperature gradient is appeared after starting impinging jet. The plate temperature is decreased over time because of the air jet, and the area of temperature gradient increased. After 2.5 second from impinging cooling, the minimum temperature was 261℃. Fig. 5 shows the temperature distribution varied with impinging angle. Fig. 5 (b) is the instantaneous temperature field at H/D=4, α=45°. Because of the impinging angle, the shape of temperature gradient is more rounded than Fig. 4 (a), and the shape of nozzle and its shade is increased. The location of UV-LED was fixed where the upper side of test section, so along the impinging angle, the overlapped nozzle area is changed including its shade. The minimum temperature after 2.5 seconds at the Fig. 4 (b) is 250.6℃, and it is lower than 30°. It is because of that even though the flow rate is same, but the vertical component of air jet to the plate is increased by the increment of impinging angel. Fig. 4 (c) is the instantaneous temperature field at H/D=4, α=60°. Because of the angle increase, the shape of temperature gradient is the most rounded, and the minimum temperature after 2.5 seconds at the Fig. 4 (c) is 232℃. Fig. 5 shows the instantaneous temperature fields which are obtained at the same impinging angle but different H/Ds. Comparing with three results, the location of nozzle and its shade are changed, however, the shape of temperature distribution remains almost same.

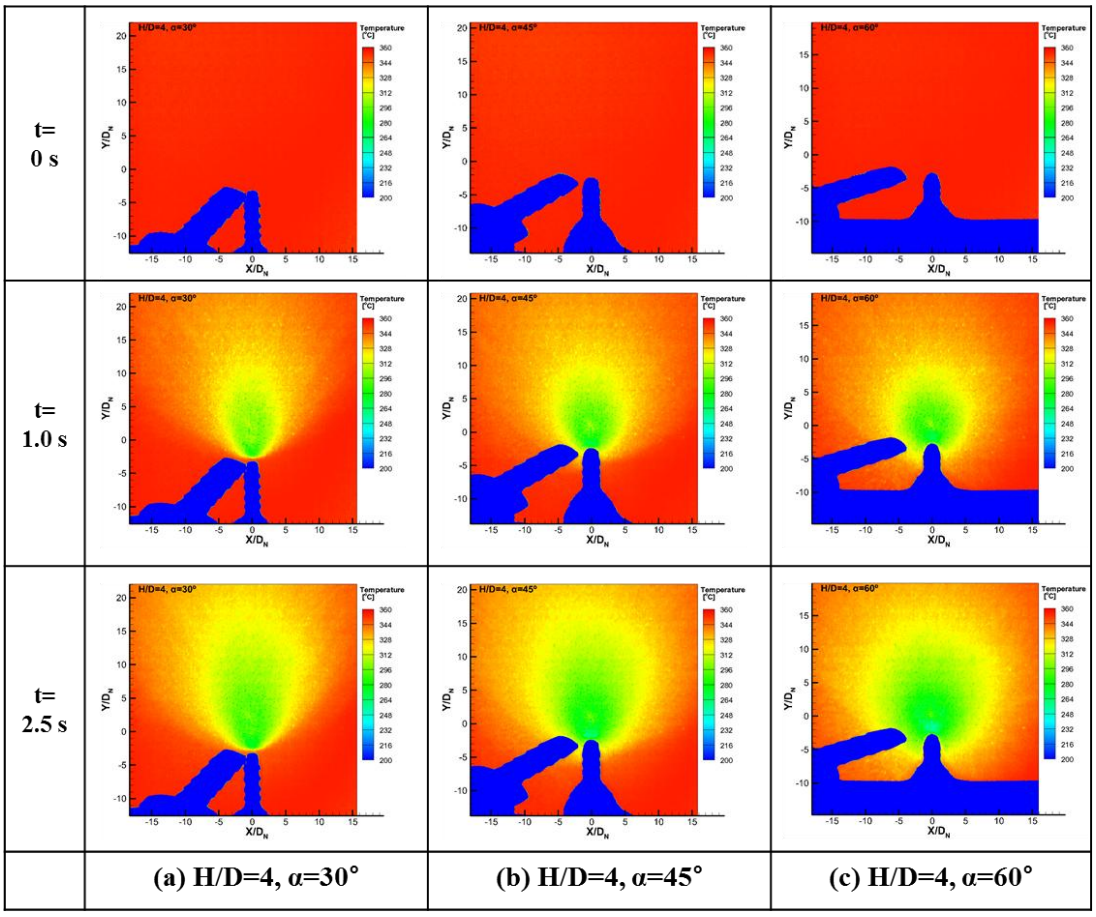

Fig. 4. Instantaneous 2D temperature fields with time; (a) H/D=4, α=30°, (b) H/D=4, α=45°, (c) H/D=4, α=60°

4.2 Heat transfer characteristic

In order to compare heat transfer characteristics depending on H/D from the nozzle to the impinging plate and impinging angles, the line data at $X/D_N = 0$ which is the direction of impinging jet were extracted. In Fig. 6, the changes of Nusselt number depending on H/D and α are demonstrated. As time passed, heat transfer gradually decreases, and the decrement quantity of heat transfer also decreases as time passed. It means that it goes toward the steady state. Generally, vertical impinging jet reaches the peak of heat transfer at the center of geometric center, however, the oblique impinging jet does not reach the peak of heat transfer at the geometric center. Instead, it reaches the peak of heat transfer at $Y/D_N < 0$. In case of oblique impinging jet, the stagnation point is located at the opposite direction of flow from the geometric center, so its peak of heat transfer is reached at the stagnation point. From the stagnation point, heat transfer rapidly decreases along $Y/D_N < 0$ whereas it relatively decreases slowly along $Y/D_N > 0$. It turns out the development of wall jet boundary layer is enhanced toward the direction of flow by the impinging angle.

Fig. 6 shows the heat transfer characteristics by variation of impinging angle at H/D = 4. At the fixed H/D, overall heat transfer increases as impinging angle increases and the secondary peak of heat transfer is reached toward the direction of flow ($Y/D_N > 0$). When jet from nozzle impinges against plate and being out, boundary layer is created, and at some point, flow of internal boundary layer is transited into laminar to

turbulent flow and strong turbulence is generated. It results in the section where heat transfer effect increases rapidly. For this reason, the secondary peak of heat transfer is affected by transition of wall jet boundary layer.

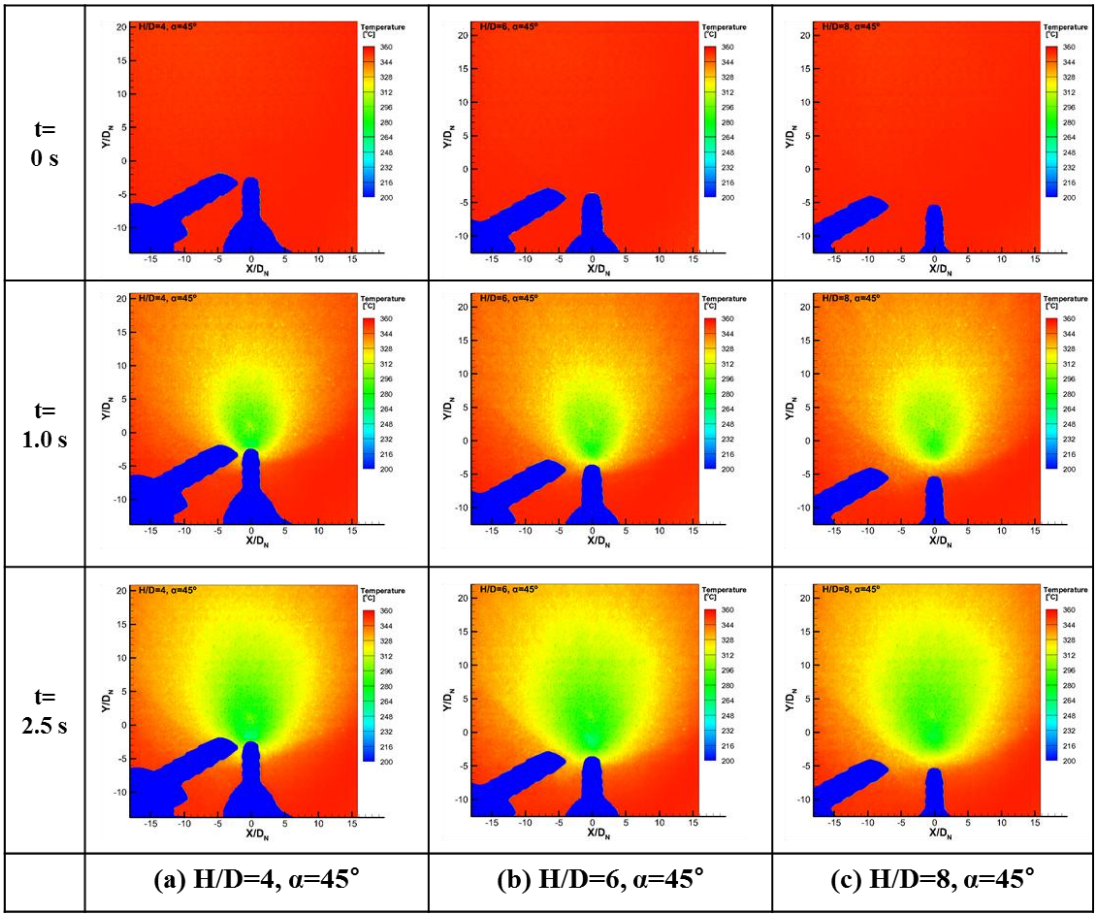

Fig. 5. Instantaneous 2D temperature fields with time; (a) H/D=4, α=45°, (b) H/D=6, α=45°, (c) H/D=8, α=45°

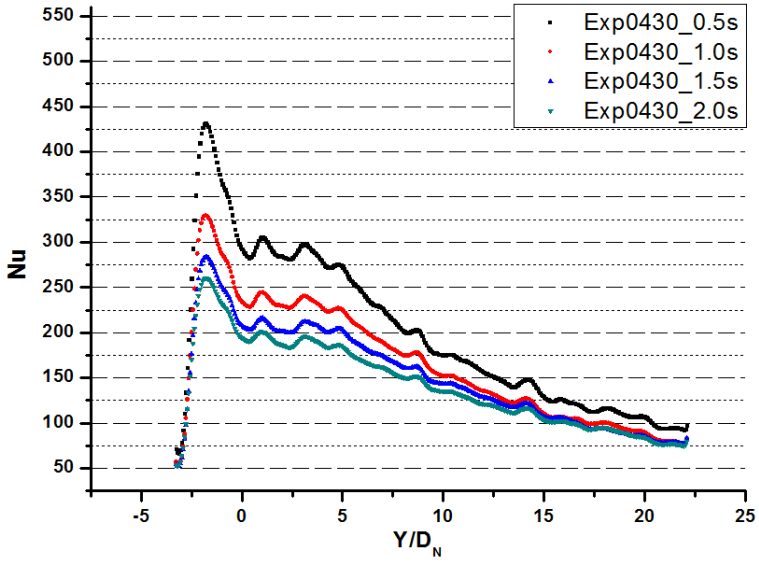

Fig. 6 (a) Nu distribution at H/D=4, α=30°

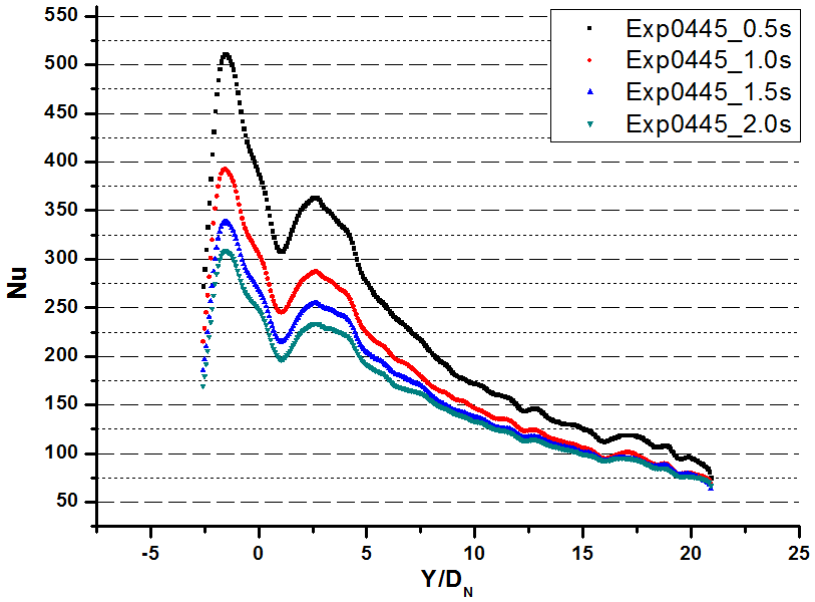

Fig. 6 (b) Nu distribution at H/D=4, α=45°

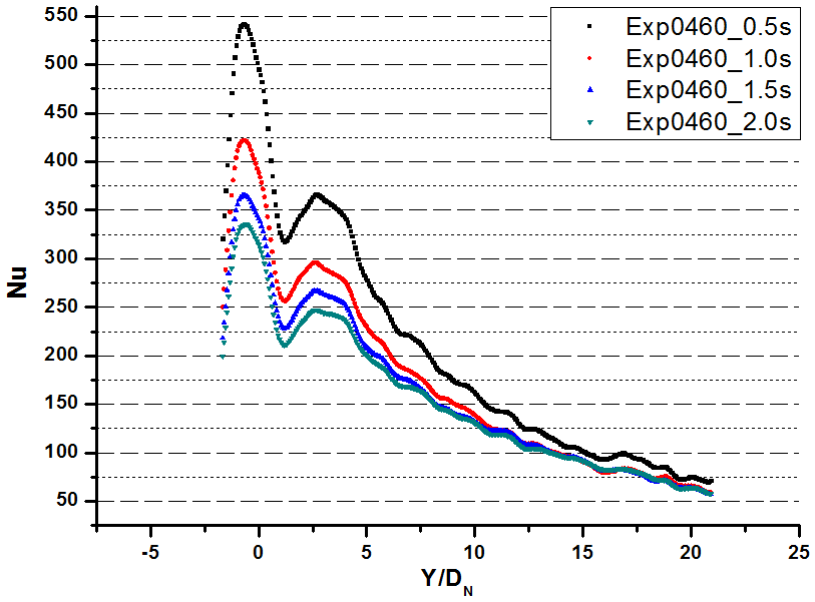

Fig. 6 (c) Nu distribution at H/D=4, α=60°

5 Conclusions

In this paper, the heat transfer characteristics of oblique impinging jet were investigated by the constructed thermographic phosphor system. 1D semi-infinite solid model was used to obtain local heat transfer coefficient and transient heat transfer characteristics were investigated. The most salient feature of transient heat transfer characteristics is that the overall heat transfer is significantly higher compared to that of the steady state. The peak heat transfer was occurring at the stagnation point, and secondary peak was also occurred at the low H/D and high impinging angle condition. These secondary peaks are occurring by transition of the wall jet boundary layer. When the distance from nozzle to plate is fixed, the air jet with high

impinging angle affect to the large area and cooling performance is also enhanced. Furthermore, when impinging angle is fixed, the minimum temperature is lower if H/D is lower. It is because of the jet potential core length, and in case of impinging jet, potential core length determined the condition that impinging jet delivered to plate, and it has a huge impact on heat transfer.

ACKNOWLEDGEMENT

This work was supported by the Energy Efficiency & Resources Core technology Program of the Korea Institute of Energy Technology Evaluation and Planning (KETEP) granted financial resource from the Ministry of Trade, Industry & Energy, Republic of Korea (No. 20112010100030).

References

[1] K. Ferrari, N. Lior, J. Slycke, An evaluation of gas quenching of steel rings by multiple-jet impingement, J Mater Process Tech, 136(1-3) (2003) 190-201.
[2] F. Hoefler, S. Schueren, J. von Wolfersdorf, S. Naik, Heat transfer characteristics of an oblique jet impingement configuration in a passage with ribbed surfaces, Journal of Turbomachinery, 134(3) (2012) 031022.
[3] B.R. Hollworth, M. Durbin, Impingement Cooling of Electronics, J Heat Trans-T Asme, 114(3) (1992) 607-613.
[4] S.V. Garimella, B. Nenaydykh, Nozzle-geometry effects in liquid jet impingement heat transfer, Int J Heat Mass Tran, 39(14) (1996) 2915-2923.
[5] S. AshforthFrost, K. Jambunathan, Effect of nozzle geometry and semi-confinement on the potential core of a turbulent axisymmetric free jet, Int Commun Heat Mass, 23(2) (1996) 155-162.
[6] M.D. Limaye, P. Gulati, R.P. Vedula, S.V. Prabhu, Effect of the profile of a convergent nozzle on heat transfer distribution of a flat plate impinged by an under-expanded jet, Exp Therm Fluid Sci, 45 (2013) 75-91.
[7] S. Roy, P. Patel, Study of heat transfer for a pair of rectangular jets impinging on an inclined surface, Int J Heat Mass Tran, 46(3) (2003) 411-425.
[8] A.A. Tawfek, Heat transfer studies of the oblique impingement of round jets upon a curved surface, Heat Mass Transfer, 38(6) (2002) 467-475.
[9] J. Brubach, A. Dreizler, J. Janicka, Gas compositional and pressure effects on thermographic phosphor thermometry, Meas Sci Technol, 18(3) (2007) 764-770.
[10] J. Brubach, J. Janicka, A. Dreizler, An algorithm for the characterisation of multi-exponential decay curves, Opt Laser Eng, 47(1) (2009) 75-79.
[11] D.L. Beshears, G. Capps, M.R. Cates, C.M. Simmons, S. Schwenterly, Laser-induced fluorescence of phosphors for remote cryogenic thermometry, Proc. SPIE Fiber Optic Smart Structures and Skins III, 1370 (1990).
[12] J. Brubach, J. Zetterberg, A. Omrane, Z.S. Li, M. Alden, A. Dreizler, Determination of surface normal temperature gradients using thermographic phosphors and filtered Rayleigh scattering, Appl Phys B-Lasers O, 84(3) (2006) 537-541.
[13] J.H. Bell, E.T. Schairer, L.A. Hand, R.D. Mehta, Surface pressure measurements using luminescent coatings, Annual Review of Fluid Mechanics, 33 (2001) 155-206.
[14] A.H. Khalid, K. Kontis, 2D surface thermal imaging using rise-time analysis from laser-induced luminescence phosphor thermometry, Meas Sci Technol, 20(2) (2009).
[15] S.J. Yi, H.D. Kim, K.C. Kim, Decay-slope method for 2-Dimensional temperature field measurement using thermographic phosphors, Exp Therm Fluid Sci, (2014).